Eur. Phys. J. D **9**, 513–516 (1999)

THE EUROPEAN PHYSICAL JOURNAL D

EDP Sciences

$AuSb_2$ alloy formation on HOPG by successive deposition of Sb clusters and Au atoms

D. Besson[1], M. Treilleux[1], A. Hoareau[1], L. Bardotti[1], B. Prével[1], A. Perez[1], and C. Esnouf[2]

[1] Département de Physique des Matériaux, Université Claude Bernard Lyon 1, 43 Bd du 11 novembre 1918, F-69622 Villeurbanne Cedex, France
[2] INSA, Laboratoire GEMPPM, Bât 502, 20 av. Albert Einstein, F-69621 Villeurbanne Cedex, France (e-mail: dbesson@dpm.univ-lyon1.fr)

Received: 31 August 1998 / Received in final form: 9 December 1998

Abstract. The behaviour of gold atoms that alloy into amorphous antimony (aSb) islands is studied by transmission electron microscopy (TEM), selected-area electron diffraction (SAED), and energy dispersive X-ray spectroscopy (EDS). In a first step, antimony thin films are produced by low-energy cluster beam deposition (LECBD). The antimony clusters (of diameter ≈ 5 nm, with 2300 atoms) are generated in a thermal source by the gas aggregation technique and deposited onto highly-oriented pyrolitic graphite (HOPG). For cluster submonolayer coverage (< 0.2 M.L.), the diffusion and interaction of clusters on substrate lead to the formation of amorphous ramified Sb islands, formed by the aggregation of spherical particles about 10 nm in diameter. In a second step, gold is vapour-deposited onto the aSb–HOPG substrate. The influence of gold atom deposition on the morphology of the islands is studied. Moreover, varying the gold thickness, we characterize the $AuSb_2$ alloy formation.

PACS. 61.46.+w Clusters, nanoparticles, and nanocrystalline materials – 61.16.Bg Transmission, reflection and scanning electron microscopy (including EBIC) – 61.82.Bg Metals and alloys

1 Introduction

The growth of thin films and nanostructures represents one of the most powerful ways to synthesize new materials with interesting properties [1, 2]. It has been shown that specific features (electronic, magnetic, optical, etc.) of small particles (with diameters in the nanometer range) are usually different from the bulk ones. In the field of chemical properties, Hashimoto and Yasuda *et al.* have shown that when foreign atoms are vapour-deposited onto nanometer-sized particles, spontaneous alloys can be formed at room temperature [3, 4]. Each study has been performed with different systems (In−Sb, Au−Sb, Al−Sb, etc.) and realized by atomic or molecular evaporation onto amorphous carbon. Antimony molecular deposition (Sb_4) leads to the formation of isolated, compact, and amorphous small islands by molecular diffusion. In a second step, evaporation of metallic atoms onto the sample leads to spontaneous alloying (crystallized or amorphous). In the specific case of gold atoms evaporated onto antimony clusters, crystallized $AuSb_2$ alloy is obtained [5, 6]. Nevertheless, gold atom diffusion is limited by the amorphous carbon substrate; thus only a few gold atoms diffuse toward the antimony particles, whereas the others collide with each other during their diffusion and create pure gold islands. Consequently, the deposit is composed of alloy and pure gold-supported particles.

In this paper, we present in Sect. 2 a new way to form (by successive deposition of antimony clusters and gold atoms) an $AuSb_2$ alloy at room temperature without any gold-supported particles on the substrate. In this work antimony thin submonolayer films are produced by LECBD. Previous theoretical and experimental studies on the nucleation and growth of thin antimony cluster films on highly-oriented pyrolitic graphite (HOPG) [7–9] have shown the number of islands at saturation scales as $(F/D)^{\frac{1}{3}}$ where F is the incident cluster flux and D the diffusion coefficient. Then, by changing the cluster flux F or the diffusion coefficient D (by varying the substrate temperature), one can adjust the saturation island density. So, on this system (aSb–HOPG), we are able to predict the antimony island density and morphology on the surface by control of the mean thickness, the substrate temperature, and the deposition rate. In order to form the $AuSb_2$ alloy on an HOPG substrate without any gold-supported particle formation, every gold atom has to diffuse toward the antimony islands. According to the nucleation and growth theories [10, 11], this required condition will be fulfilled if the density of gold-supported particles on a free-of-defects HOPG substrate is lower than the antimony island one. Then the Sb islands on the substrate act as defects, and gold atoms are trapped by these defects. A gold deposition using a spiral-shaped tungsten filament heated by Joule effect satisfies this requirement.

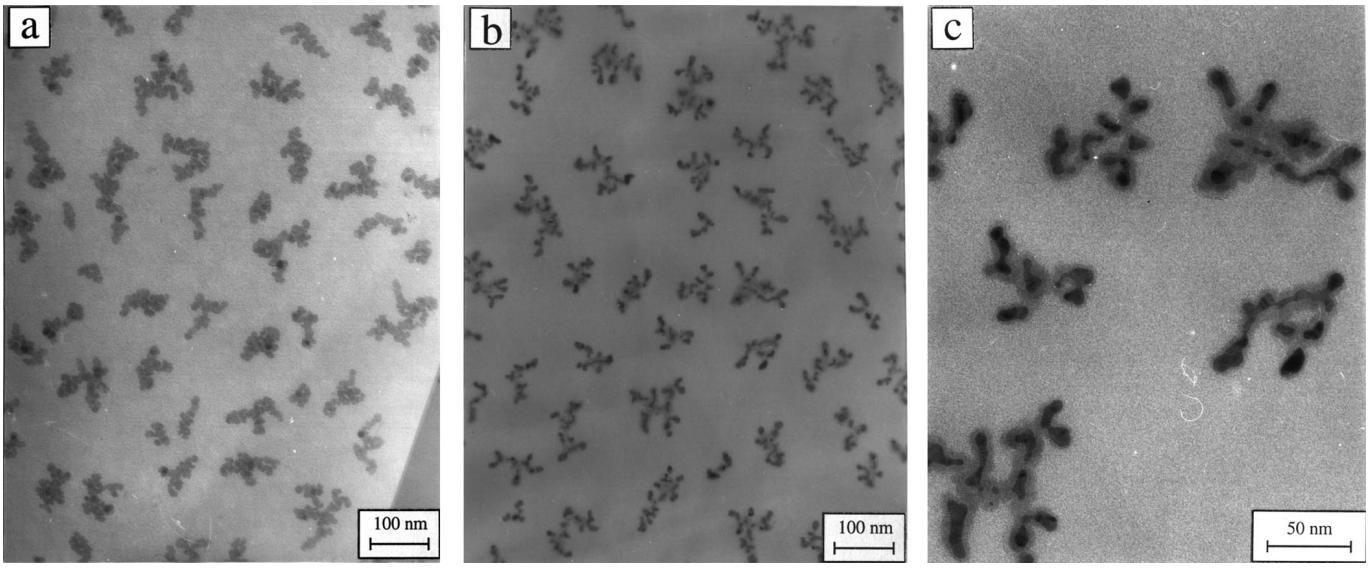

Fig. 1. (a) TEM micrograph of Sb deposit obtained by LECBD of antimony clusters (mean diameter of incident clusters: 5.4 nm; deposition rate: 0.071 $\mathrm{nm \cdot s^{-1}}$; mean thickness: 0.5 nm) on HOPG at 308 K. (b) TEM micrograph of (Au–Sb) deposit obtained by post-deposition of gold atoms from a tungsten filament (deposition rate: 0.002 $\mathrm{nm \cdot s^{-1}}$; mean thickness: 0.2 nm) on the previous aSb–HOPG substrate at 308 K. (c) Enlargement of (b)

In Sect. 3, the evolution of the morphology of the islands and the alloy formation versus deposited gold thickness are presented and discussed.

2 Experimental procedure

Before deposition, in order for the surface to be cleaned, the graphite samples are freshly cleaved in air and annealed at 773 K for 5 h in the deposition chamber where the pressure is less than 10^{-4} Pa. A reference temperature $T_S = 308$ K is chosen for the deposition. Thin antimony films are produced by LECBD. The antimony cluster beam is generated by the gas-aggregation technique in a source similar to that developed by Sattler *et al.* [12]. The metallic vapour obtained from a heated crucible is condensed in an inert Ar gas and cooled at liquid–nitrogen temperature. The cluster size is controlled by the inert-gas pressure and measured by a time-of-flight mass spectrometer. In the present work, the size distribution of the incident antimony clusters is centered on 2700 atoms, corresponding to a mean diameter of 5.4 nm, assuming a spherical shape for the free clusters. The deposition rate and the thickness are monitored by a crystal-quartz monitor located close to the substrate. In this study, the equivalent thickness is fixed at 0.5 nm (corresponding to a 0.15 monolayer) in order to reach the maximum island density (8×10^9 islands $\cdot$ $\mathrm{cm^{-2}}$ at 308 K for a deposition rate of 0.071 $\mathrm{nm \cdot s^{-1}}$).

Then gold is evaporated onto the substrate in the same deposition chamber using a spiral–shaped tungsten filament. As for antimony cluster deposition, evaporation rate and thickness are monitored by a crystal-quartz monitor. Samples with different gold thicknesses have been elaborated in order to examine structural and morphological evolutions. Observations and energy dispersive X-ray spectroscopy (EDS) analysis are realized *ex situ* 24 h after the deposition with a TOPCON electron microscope operating at an accelerating voltage of 120 kV or 200 kV. Moreover, EDS characterizations are used to determine the average composition of antimony and gold, and consequently allow one to deduce the sticking coefficient of gold atoms on aSb–HOPG.

3 Results and discussion

3.1 Efficiency of the technique

Figure 1a shows the morphology of the antimony deposit on HOPG (mean thickness of 0.5 nm). The islands are ramified, and their sizes range from 30 to 200 nm. They are composed by the aggregation of spherical amorphous antimony particles of about 10 nm in diameter. The island density is 8×10^9 islands $\cdot$ $\mathrm{cm^{-2}}$, in agreement with previous results [7, 8]. After a deposition of gold atoms ($0.002\ \mathrm{nm \cdot s^{-1}}$ deposition rate and 0.2 nm thickness), the density and shape of ramified islands are not modified (Fig. 1b). Figure 1c presents an enlargement of Fig. 1b. One can notice that the contrast in the core of the particles has increased due to their crystallization. More details will be given in the next sub-section.

Moreover, gold atoms are not observed on the HOPG substrate as individual Au-supported particles between ramified islands. This result was expected, since previous experiments have shown that the gold island density on a free-of-defects HOPG substrate is 5.7×10^9 islands $\cdot$ $\mathrm{cm^{-2}}$ (lower than the one of antimony ramified islands: 8×10^9 islands $\cdot$ $\mathrm{cm^{-2}}$), and that the gold particles' sizes

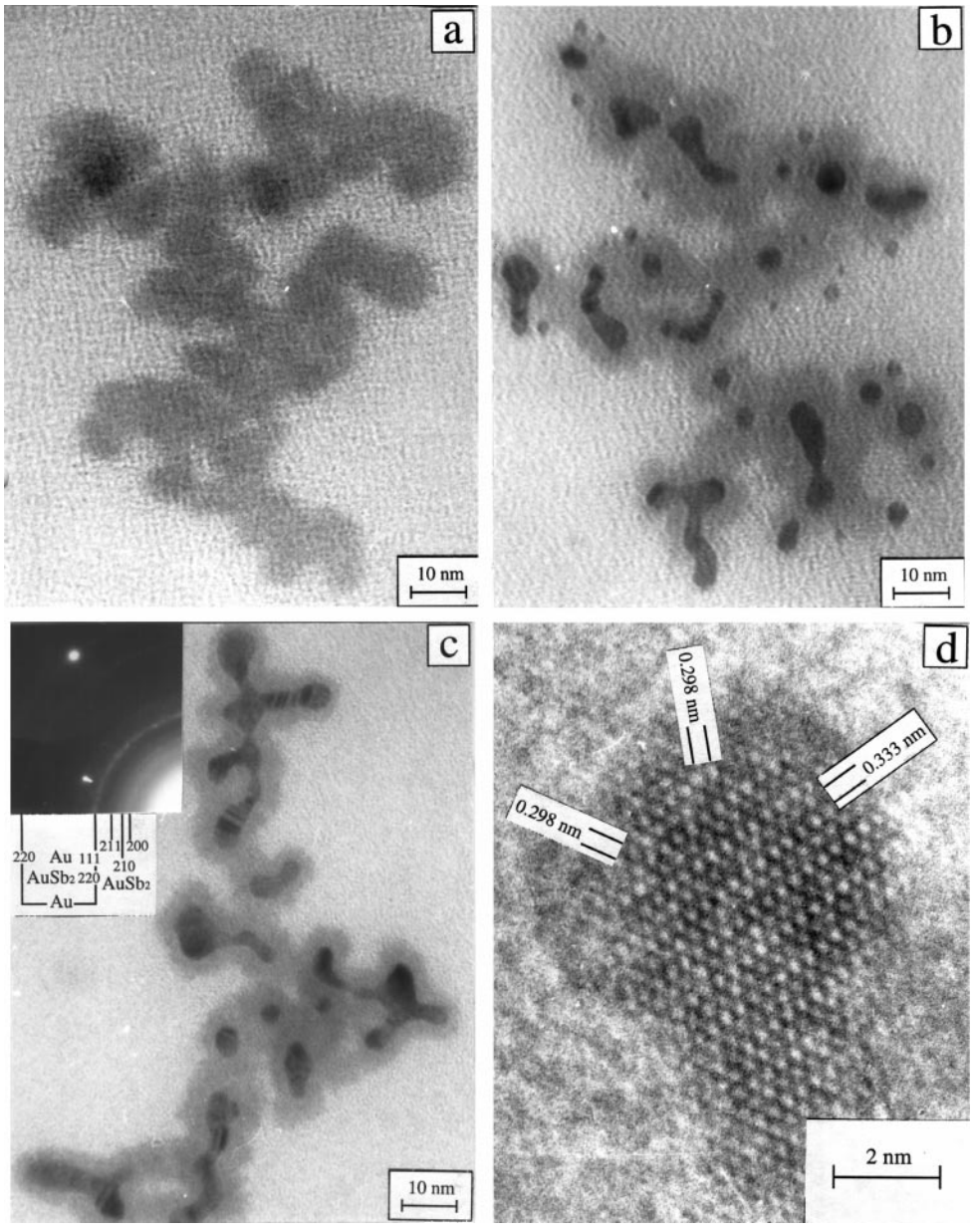

Fig. 2. TEM micrographs of ramified islands on HOPG obtained by LECBD of antimony clusters (mean diameter: 5.4 nm; deposition rate: $0.071\,\mathrm{nm\cdot s^{-1}}$; mean thickness: 0.5 nm) and after deposition of gold atoms from a tungsten filament (deposition rate: $0.002\,\mathrm{nm\cdot s^{-1}}$). $T_S = 308$ K. (a) Pure Sb island. (b) Au-Sb island (gold equivalent thickness 0.1 nm, i.e., 26% in gold atomic concentration). (c) Au–Sb island (gold equivalent thickness 0.14 nm, i.e., 33% in gold atomic concentration). The insert shows a SAED performed on a large area of the sample. (d) HRTEM image of $AuSb_2$ crystallized domain obtained after deposition of 0.2 nm gold-equivalent thickness (i.e., 42% in gold atomic concentration). Fringes corresponding to interplanar distances of 0.298 nm and 0.333 nm are observed. The $AuSb_2$ particle is observed in the [001] direction.

range from 30 to 40 nm for these deposition conditions [13]. Notice that when we use a Knudsen cell, heated by electronic bombardment, for gold deposition onto an HOPG substrate under the same evaporation conditions ($0.002\,\mathrm{nm\cdot s^{-1}}$ deposition rate and 0.2 nm thickness), the gold island density is 2×10^{12} islands$\cdot\,\mathrm{cm^{-2}}$ and the particles' sizes range from 0.8 to 2.5 nm. This high density is the result of the nucleation on defects created on the HOPG surface by energetic gold ions present in the beam during the evaporation [13].

3.2 $AuSb_2$ alloy formation

The second step is to understand if there is a required condition in for synthesizing the alloy. For instance, is there a critical gold thickness $(t_{Au})_c$ for alloy formation?

Since the stoichiometric alloy composition is $AuSb_2$, we can calculate the mean gold thickness t_{Au} required to obtain supported islands composed exclusively of this alloy. Considering the bulk atomic concentration of Au and Sb ($C_{Au} = 5.9\times10^{28}\,\mathrm{atoms\cdot m^{-3}}$ and $C_{Sb} =$

3.31×10^{28} atoms $\cdot$ m^{-3}, respectively) and neglecting any evaporation process, t_{Au} is given by the formula $t_{Au} = \frac{C_{Sb}}{C_{Au}} \frac{t_{Sb}}{2}$ where t_{Sb} is the antimony mean thickness (0.5 nm). Then the $AuSb_2$ composition corresponds to $t_{Au} = 0.14$ nm. Three samples have been prepared under the same conditions (substrate temperature $T_S = 308$ K, antimony cluster deposition rate of $0.071\,\text{nm}\cdot\text{s}^{-1}$, gold atom deposition rate of $0.002\,\text{nm}\cdot\text{s}^{-1}$). The gold mean thicknesses were 0.1, 0.14, and 0.2 nm. First we must verify that no gold or antimony evaporation on the HOPG substrate occurs during thin film formation. In the case of antimony cluster deposition, previous results [8] have shown that the sticking coefficient is 1 for Sb clusters on HOPG. In order to evaluate what happens for gold deposition, we have made a comparison between the Au atomic concentration on the surface, calculated from the mean thicknesses obtained by a crystal-quartz monitor, and an EDS analysis performed on a large area. The agreement of better than 10% between the two methods suggests that there is no gold evaporation on the aSb–HOPG substrate kept at 308 K.

Figure 2a–c show TEM images revealing the evolution of the morphology of an island with an Au-deposited mean thickness (0, 0.1 and 0.14 nm). For the 0.1 nm mean thickness (Fig. 2b), isolated and crystallized domains appear inside the island, whereas the outer part keeps an amorphous structure. For the higher thickness 0.14 nm(Fig. 2c), the size of the crystallized domains increases, and they become nearly continuous in the core of the ramified island. The SAED pattern, performed on a large area of the sample is shown in Fig. 2c. One can observe small dots corresponding to HOPG, and rings corresponding to interplanar distances $d = 0.333$ nm, 0.298 nm and 0.272 nm, characteristics of $AuSb_2$ and $d = 0.236$ nm which can be assigned to $AuSb_2$ and Au. These rings confirm the presence of alloy. Faint rings are also observed for the 0.1 nm-thickness specimen at the same positions. The alloy formation is also confirmed by high resolution transmission electron microscopy (HRTEM) (Fig. 2d) and by optical diffraction on the negative HRTEM micrograph. Two systems of fringes corresponding to (210) planes ($d = 0.298$ nm) and another one corresponding to (200) planes ($d = 0.333$ nm) are observed on the micrograph. The $AuSb_2$ particle is observed in the [001] direction.

All these observations clearly indicate that gold atoms deposited on aSb–HOPG (without re-evaporation) diffuse toward the amorphous antimony ramified islands and dissolve. Small isolated and crystallized domains are created in the center of the islands. As the deposited gold thickness increases, the domains develop and merge. At high gold concentration, the islands are probably formed by a mixture of crystallized $AuSb_2$ alloy and Au plus amorphous antimony or amorphous Au–Sb alloy. These preliminary results show that the $AuSb_2$ alloy can be formed using these deposition techniques, but much has to be done in order for a deeper understanding of the islands' structure to be gained. For instance, we plan to realize concentration profiles of an island in order to know more precisely the composition of a gold–antimony island.

4 Conclusion

Alloying behaviour of gold atoms into antimony particles has been studied by TEM, HRTEM, and EDS. Sb particles were prepared by low-energy Sb cluster beam deposition on HOPG at 308 K, which led to the formation of ramified islands made by the juxtaposition of spherical Sb amorphous particles of about 10 nm in diameter. Then, using a tungsten filament, gold atoms were evaporated onto the aSb–HOPG sample at 308 K. All gold atoms can diffuse toward Sb islands without evaporation. We have shown that $AuSb_2$ alloy domains are formed in the core of the antimony island by spontaneous dissolution. However, when the gold concentration surpasses the one corresponding to the $AuSb_2$ composition, do not know for certain whether the supported islands are composed exclusively by $AuSb_2$ alloy or other phases such as pure Au or amorphous Sb are still present. This will be analyzed in the next step of the study.

References

1. See, for example, F. Capasso (Ed.): *Physics of Quantum Devices* (Springer, Berlin 1990)
2. P. Jensen: La Recherche **283** , 42 (1996)
3. M. Hashimoto: J. Cryst. Growth **79**, 140 (1986)
4. H. Yasuda, H. Mori, T. Muraki, T. Sakata: Z. Phys. D **31**, 209 (1994)
5. H. Yasuda, H. Mori: Mater. Sci. Eng. A **217/218**, 244 (1996)
6. H. Yasuda, H. Mori: Thin Solid Films **298**, 143 (1997)
7. L. Bardotti, P. Jensen, A. Hoareau, M. Treilleux, B. Cabaud: Phys. Rev. Lett. **74**, 4694 (1995)
8. L. Bardotti, P. Jensen, A. Hoareau, M. Treilleux, B. Cabaud, A. Perez, F. Cadete Santos Aires: Surf. Sci. **367**, 276 (1996)
9. P. Jensen, A.-L. Babarasi, H. Larralde, S. Havlin, H.E. Stanley: Phys. Rev. B **50**, 15 316 (1994)
10. S. Stoyanov, D. Kaschiev: *Current Topics in Materials Science*, ed. by E. Kaldis, vol. 7 (North-Holland, Amsterdam 1981)
11. J. Villain, A. Pimpinelli, L.-H. Tang, D.E. Wolf: J. Phys. I (France) **2**, 2107 (1992)
12. K. Sattler, J. Muhlbach, R.E. Recknagel: Phys. Rev. Lett. **45**, 821 (1980)
13. D. Besson, L. Bardotti, A. Hoareau, B. Prével, M. Treilleux, A. Perez, C. Esnouf: Mater. Sci. Eng. B **60**, 51 (1999)